



Syntheses and Crystal Structures of the New Ag–S Clusters

[Ag₇₀S₁₆(SPh)₃₄(PhCO₂)₄(triphos)₄] and [Ag₁₈₈S₉₄(PR₃)₃₀]**

Xiu-Jian Wang, Timo Langetepe, Claudia Persau, Bei-Sheng Kang, George M. Sheldrick, and Dieter Fenske*

Dedicated to Professor Achim Müller on the occasion of his 65th birthday

Many investigations towards synthesis and structural characterization of large metal-rich clusters have been reported over the last few years. Particularly noteworthy are the oxometallates of molybdenum described by Müller et al.; only recently Na₄₈[H₃Mo₃₆₈O₁₀₃₂(H₂O)₂₄₀(SO₄)₄₈]·*n* 1000H₂O (*x* ≈ 16; *n* ≈ 1000), the largest known derivative of a heteropolyacid was structurally characterized.^[1] Other examples of large cluster complexes are [Pd₁₄₅(CO)_x(PET₃)₃₀] (*x* ≈ 60) made by Dahl et al.^[2] and [Ga₃₄N(SiMe₃)₂]₂₀Li₆Br₂(thf)₂₀ reported by Schnöckel and Schnepf.^[3] The synthesis of the larger Ag–S cluster complexes [Ag₁₄S(SPh)₁₂(PPh₃)₈]^[4] and [HNet₃]₄–[Ag₅₀S₇(SC₆H₄tBu)₄₀]^[5] was recently achieved by Jin et al.

Over the last few years one of our major fields of interest was the synthesis of transition-metal clusters containing S, Se, Te, P, As, and Sb as bridging ligands, for example, copper-chalcogenide clusters stabilized by tertiary phosphane ligands.^[6] Reactions of transition-metal salts with Group 16 silyl derivatives E(SiMe₃)₂ or RESiMe₃ (R = alkyl- or aryl-; E = S, Se, Te) allows access to these clusters.^[7] Addition of tertiary phosphanes to these reactions prevents the formation of the thermodynamically stable binary phase.^[8]

Compounds obtained by this route include: [Cu₁₄₆Se₇₃–(PPh₃)₃₀],^[9] [Ag₁₇₂Se₄₀(SenBu)₉₂(dppp)₄]^[10] (dppp = bis(1,3-diphenylphosphanyl)propane), [Ag₃₈Te₁₃(TerBu)₁₂(dppe)₆] (dppe = bis(1,2-diphenylphosphanyl)ethane),^[11] [Au₁₈Se₈–(dppe)₆]Cl₂^[12], and [Zn₁₆Te₁₃(TePh)₆(tmeda)₅]^[13] (tmeda = tetramethylethylenediamine). Herein we report the synthesis of the Ag–S clusters **1**, **2**, and **3** containing 120 and 282 heavy atoms, respectively, in the cluster core.

[Ag₇₀S₁₆(SPh)₃₄(PhCO₂)₄(triphos)₄] **1**

[Ag₁₈₈S₉₄(PnPr₃)₃₀] **2**

[Ag₁₈₈S₉₄(PnBu₃)₃₀] **3**

The reaction of a suspension of silver benzoate and triphos [1,1,1-tris[(diphenylphosphanyl)methyl]ethane] with a mixture of S(Ph)SiMe₃ and S(SiMe₃)₂ (2:1) at –20 °C in diglyme produces a deep red solution from which small red needles of **1** [Eq. (1)], can be isolated.



Reaction of S(SiMe₃)₂ with silver trifluoroacetate and PnPr₃ at –40 °C in diglyme initially produces a red solution. After a few hours stirring, the reaction is allowed to warm up to room temperature. The solution becomes dark and black crystals of **2** are formed [Eq. (2)]. Employment of PnBu₃ in an analogous reaction produces black crystals of **3** [Eq. (2)]. Depending on the reaction conditions, **2** is often produced together with black amorphous Ag₂S. Attempts to recrystallize **2** and **3** from THF or CH₂Cl₂ failed and produced Ag₂S as the only isolatable material. The different colors of **1** and **2** (red and black) arise from quantum size effect, which result from the dependency of the band gap on particle size.^[14]



The molecular structures of complexes **1** and **2** in the solid-state were determined by X-ray crystallography.^[15] Compound **1** crystallizes in the space group *P* $\bar{1}$ with two molecules in the unit cell. The molecular structure is shown in Figure 1. The cluster core consists of an arrangement of 70 silver and 50 sulfur atoms protected by four triphos ligands and 34 phenyl rings of SPh[–] groups. Four benzoate ligands make up the additional charge to give a neutral cluster by coordinating by their oxygen centers to the surface of the cluster core.

The sulfur atoms are arranged in a highly distorted a layer substructure (Figure 2) with no bonding interactions. The sulfur atoms of the SPh[–] groups (S1–S34; yellow) are located on the surface of the cluster and S^{2–} ligands (S35–S50; orange) are part of the inner core. The four sulfur layers are highly corrugated with a pseudo S₄ axis through the midpoints of S39–S47 and S14–S45 (in Figure 2 from bottom to top). The top and bottom sulfur layers shown contain eight S atoms and are twisted by 90° relative to each other. Each of these layers contains two S^{2–} ligands (S39, S47 and S35, S45) and six SPh[–] ligands (S17, S18, S21, S24, S25, S30 and S4, S8, S11, S14, S16, S29, respectively). The two inner sulfur layers contain 17 S atoms each, six S^{2–} ligands (S36, S38, S40, S44, S46, S48 and S37, S41, S42, S43, S49, S50, respectively), which are surrounded by rings of 11 thiolato ligands (S1, S5, S7, S9, S10, S19, S20, S22, S27, S28, S34 and S2, S3, S6, S12, S13, S15, S23, S26, S31, S32, S33).

The S atoms in the SPh[–] ligands are μ₂-, μ₃-, and μ₄ bridging, whereas central S^{2–} ions act as μ₄ to μ₇ bridges between Ag

[*] Prof. Dr. D. Fenske, X.-J. Wang, Dr. T. Langetepe, Dr. C. Persau
Institut für Nanotechnologie (INT)
Forschungszentrum Karlsruhe
and
Institut für Anorganische Chemie der Universität
Engesserstrasse, Geb. 30.45, 76128 Karlsruhe (Germany)
Fax: (+49) 721-608-8440
E-mail: dieter.fenske@chemie.uni-karlsruhe.de

X.-J. Wang, Prof. Dr. B.-S. Kang
School of Chemistry and Chemical Engineering
Zhongshan Universität, Guangzhou (Volksrepublik China)
Prof. Dr. G. M. Sheldrick
Institut für Anorganische Chemie
Universität Göttingen
Tammanstrasse 4, 37077 Göttingen (Germany)

[**] This work was supported by the Deutsche Forschungsgemeinschaft (Centrum für funktionelle Nanostrukturen) and the Fond der Chemischen Industrie. R = *n*Pr, *n*Bu; triphos = 1,1,1-tris[(diphenylphosphanyl)methyl]ethane.

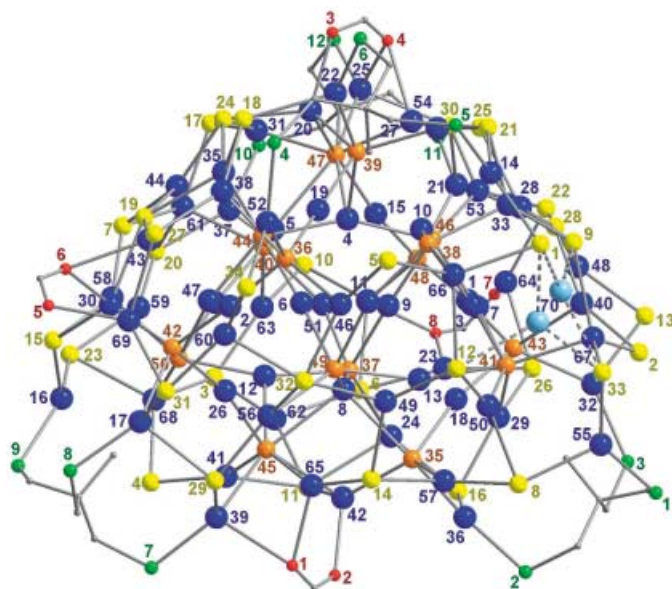


Figure 1. Molecular structure of **1** (phenyl rings of the phosphane, benzoate, and SPh[−] are omitted for clarity; P (green), S^{2−} ions (orange), S atoms of PhS[−] ligands (yellow), O (red), Ag (blue), both positions of Ag70 (light blue)). Selected bond lengths [± 0.5 pm] and angles [$\pm 0.2^\circ$]: Ag8–Ag13 288.9, Ag19–Ag22 338.0, Ag70–Ag70' 132.8, Ag1–S43 237.0, Ag7–S43 289.6, Ag13–S41 251.3, Ag17–S29 275.3, Ag17–S42 260.3, Ag22–S39 242.3, Ag28–S46 292.7, Ag39–S29 279.3, Ag46–S5 242.0, Ag64–S22 249.1, Ag64–S48 292.2, Ag67–S2 246.4, Ag69–S27 266.0, Ag69–S31 244.4, Ag36–P2 239.0, Ag52–P4 246.3, Ag34–O8 258, Ag43–O6 251, Ag64–O7 229, Ag69–O5 233, S43–Ag1–S48 174.8, S44–Ag4–S46 155.3, S38–Ag10–S46 160.4, S25–Ag28–S46 81.6, S28–Ag53–S46 89.2, S20–Ag59–S23 137.5, P6–Ag22–S39 147.8, P10–Ag37–S10 94.1, O8–Ag23–S6 89.5, O5–Ag69–S31 125.0, Ag41–S4–Ag68 92.4, Ag46–S5–Ag66 85.1, Ag23–S26–Ag29 70.2, Ag49–S32–Ag60 163.3, Ag67–S33–Ag70 66.0, Ag38–S36–Ag52 68.0, Ag4–S39–Ag10 61.5, Ag4–S39–Ag22 159.8, Ag13–S41–Ag67 164.6, Ag8–S45–Ag12 63.4, Ag26–S45–Ag42 158.2.

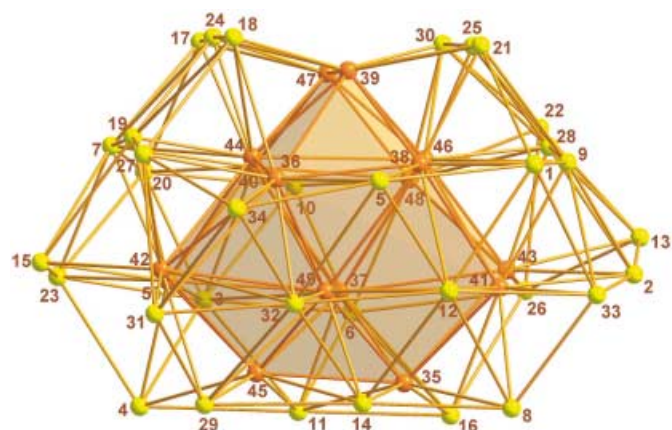


Figure 2. The sulfur substructure of **1** S atoms of PhS[−] (yellow) and polyhedral arrangement of S^{2−} ions (orange).

atoms. The P-bonded Ag atoms exhibit either a trigonal-planar (Ag14, Ag16, Ag22, Ag25, Ag32, Ag36, Ag37, Ag39, Ag52, Ag55) or a distorted-tetrahedral (Ag17, Ag21) coordination geometry. Ag atoms coordinated by O (benzoate) atoms have as analogous coordination geometry (trigonal planar for Ag23, Ag43, Ag54, Ag65, Ag69; tetrahedral for Ag20, Ag34, Ag42, Ag64). The remaining 49 Ag atoms are

solely coordinated by S^{2−} ligands and have coordination numbers from two to four. Observed S–Ag–S angles for the Ag atoms range from 137.5(2)–174.8(2) $^\circ$ (non-linear), 89.2(2)–160.4(2) $^\circ$ (trigonal planar with Σ S–Ag–S = 348.5–360.0 $^\circ$) and 81.6(2)–155.3(2) $^\circ$ (tetrahedral).

As a consequence of these different Ag coordination environments, significantly shorter Ag–S bonds (237.0(4)–251.3(4) pm) are observed for coordination number two in comparison to trigonal planar coordination (242.0(5)–289.6(4) pm) or tetrahedral coordination (246.4(7)–292.7(4) pm). Ag70 is disordered over two sites and is coordinated by S1, S33 and S9 or S12.

Assuming that in **1** only S^{2−}, SPh[−], and monoanionic benzoate ligands are present, all the Ag atoms have the formal charge +1 and thus have a d¹⁰ configuration. Ag–Ag separations within the cluster core are 288.9(2)–338.0(2) pm and indicate that there are no Ag–Ag interactions.

Compound **2** crystallizes in the space group $P\bar{1}$ with one molecule in the unit cell. The molecular structure shows **2** has an almost spherical structure with $\bar{1}$ symmetry (Figure 3). The surface is protected by 30 PnPr₃ ligands. The diameter of the Ag₂S core is 1.8–2.0 nm. On including the bound P atoms the diameter increases to 2.25–2.50 nm and when also the nPr groups are included the particle size is 3.2 nm. This size corresponds well with the hydrodynamic diameter of the particle determined by dynamic light-scattering measurements.

The structure of **2** is highly complex and in addition the Ag and S atoms in the cluster center are disordered. The extent of the disorder depends on the reaction conditions leading to the formation of **2** and on the temperature during data collection. Surprisingly, the disorder does not affect the atomic positions at the cluster periphery. In Ag₂S—an ionic conductor—a similar disorder of the Ag⁺ ions occurs at temperatures above 150 $^\circ$ C.^[16] In the solid-state structure of Ag₂S, however, only a few Ag⁺ ions show temperature-dependent disorder. Assuming that **2** is a nanoscopic section of the Ag₂S structure then it should not be surprising to make similar observations. It is, however, unusual that this observation can be made for a cluster of the size of **2**. To our surprise, it evolved that the structure of **2** cannot be interpreted as part of the Ag₂S structure. Related selenido and selenato complexes of silver (with less than 112 Ag atoms) are known to have structures composed of several shells, for example, [Ag₃₀Se₈(Se*t*Bu₁₄(PnPr₃)₈)] and [Ag₉₀Se₃₈(Se*t*Bu)₁₄(PET₃)₂₂].^[10] However, the Se atoms in [Ag₁₁₂Se₃₂(SenBu)₄₈(PrBu₃)₁₂] and [Ag₁₇₂Se₄₀(SenBu)₉₂(dppp)₄], the largest Ag₂Se cluster to be structurally characterized, adopt a distorted body-centered cubic arrangement in which the Ag atoms occupy the vacant positions and are surrounded by Se atoms in a distorted trigonal-planar or tetrahedral coordination environment. Disorder of Ag atoms, however, has also occurred in Ag₉₀[−], Ag₁₁₂[−], and Ag₁₇₂ clusters and seems to be a common feature in the structures of these clusters.

The structural change from complexes composed of several shells to structures that can be regarded as part of a solid-state structure of a binary compound very much depends on the size and properties of the cluster. These influences have already been discussed for ligand-protected M₂E clusters

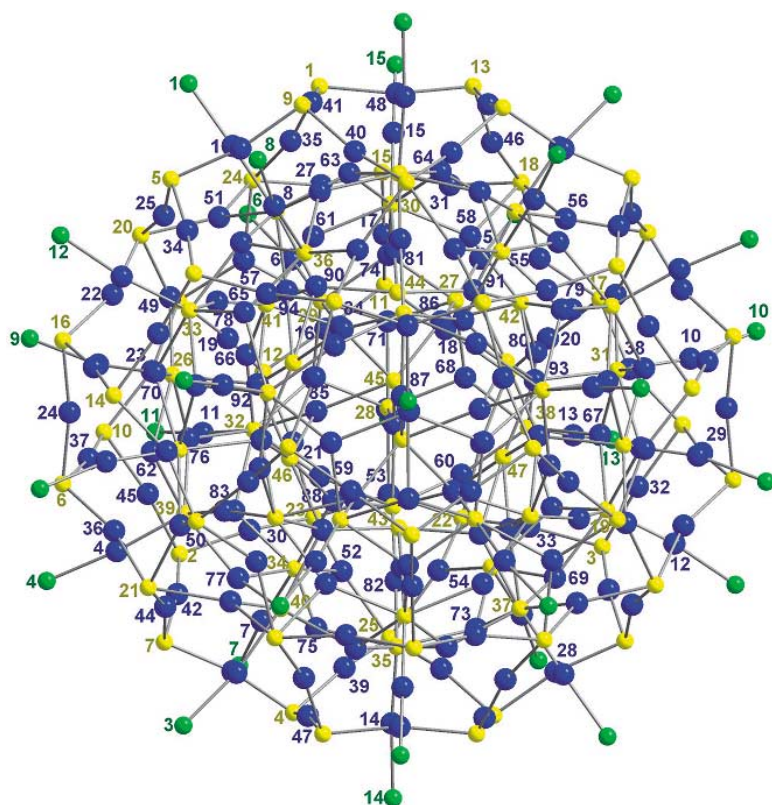


Figure 3. Molecular structure of **2** (*n*Pr groups atoms have been omitted for clarity P (green), S²⁻ ions (yellow), Ag (blue)). Selected bond lengths [± 0.8 pm] and angles [$\pm 0.3^\circ$]: Ag1–Ag25 307.3, Ag14–Ag47 287.2, Ag1–S37 244.3, Ag28–S9 239.2, Ag64–S39 265.1, Ag89–S47 242.1, Ag90–S41 272.7, Ag92–S47 280.2, Ag5–P5 236.5, Ag3–P3 241.2; S12–Ag16–S11 171.8, S21–Ag44–S7 162.0, S23–Ag53–S28 109.5, S18–Ag55–S17 137.1, P3–Ag3–S40 163.9, P11–Ag11–S32 176.1, Ag41–S1–Ag63 69.9, Ag16–S11–Ag17 99.9, Ag24–S16–Ag22 108.9, Ag77–S39–Ag76 130.4.

(E = S, Se, M = Cu, Cd).^[7–9,17,18] It is surprising in this context that the number of Ag₂E units present in a cluster does not allow any prediction of the structural change. Only recently we managed to demonstrate this for [Ag₁₂₄Se₉₇(SePrBu₂)₄Cl₆(*t*Bu₂P(CH₂)₃PrBu₂)₁₂] in which the Se substructure consists of a central Se atom surrounded by a distorted Se₁₆ Frank–Kasper polyhedron, which itself is surrounded by a Se₄₄ polyhedron as the second shell.^[18] Similar structural properties are found in **2**: 94 S atoms are distributed over three shells. The outer shell consists of 50 (S1–S25), the middle shell of 34 (S26–S42), and the inner shell of 10 (S43–S47) S atoms. Non-bonding S–S separations are in the range 450–500 pm.

Figure 4 shows the arrangement of the sulfur polyhedra in **2**. The S₅₀ polyhedron (bright yellow) consists of 30 twisted S₅ rings linked together by six S₃ triangles. The middle shell (dark yellow) forms a previously unknown Δ_3 polyhedron of 34 S atoms that itself contains an S₁₀ polyhedron (orange). However, because of the disorder, the structure of the S₁₀ polyhedron cannot be determined. During refinement comparatively high electron density remains within the cluster core; considering Ag–S bond lengths we believe that this observation can be explained by disordered Ag and S atoms. Hence, Ag atoms (Ag87–Ag94) in the vicinity of the S₁₀ polyhedron show high temperature factors. For these reasons, the formula of **2** has to be considered as idealized, but

coincides well with elemental analysis and also with interatomic distances commonly observed for Ag–S bonds. The edges of the S₅₀ outer shell are occupied by Ag atoms (Ag16–Ag48; Figure 5) which act as non-linear bridges between two S atoms (Ag–S 236.1(9)–244.2(8) pm, S–Ag–S: 155.3(2)–172.2(3) $^\circ$).

The shortest Ag–S separations are observed in the middle S₃₄ shell are in the range 333–388 pm. These very weak interactions could be the reason for the uncommon S–Ag–S bond angles in the outer shell. The broad range of Ag–E distances (E = S, Se, Te), generally complicates the structural discussion of Ag–chalcogenide clusters. The atoms Ag49–Ag57 are each coordinated by two outer-shell S atoms and act as bridging atoms between the outer shell (S₅₀ polyhedron) and the middle shell (S₃₄ polyhedron). Thus the atoms Ag49–Ag57 are surrounded by S atoms in a distorted trigonal-planar or tetrahedral fashion (S–Ag–S 104.3(2)–137.1(3) $^\circ$, Σ S–Ag–S 353.2–357.9 $^\circ$). The Ag–S bond lengths are between 247.2(8) and 283.5(8) pm. Additional weak interactions with outer-shell S atoms range from 301–309 pm.

Figure 5 shows an Ag₁₁₄S₅₀ polyhedron (Ag1–Ag57 and S1–S25) constructed from 30 Ag₅S₅-ten-membered rings. One Ag atom (Ag1–Ag15), stabilized by a phosphane (PnPr₃) ligand, caps each ring, these Ag atoms are not coordinated by S atoms of the S₅₀ shell but to 30 S atoms of the middle S₃₄ polyhedra. (Figure 6 shows the distorted linear coordination of Ag1–Ag15 by the S atoms the PnPr₃ ligands Ag–P 236.5(7)–241.2(7) pm, Ag–S 239.1(6)–244.7(5) pm, P–Ag–S 163.9(3)–176.1(2) $^\circ$). There are no interactions between Ag1–Ag15 and

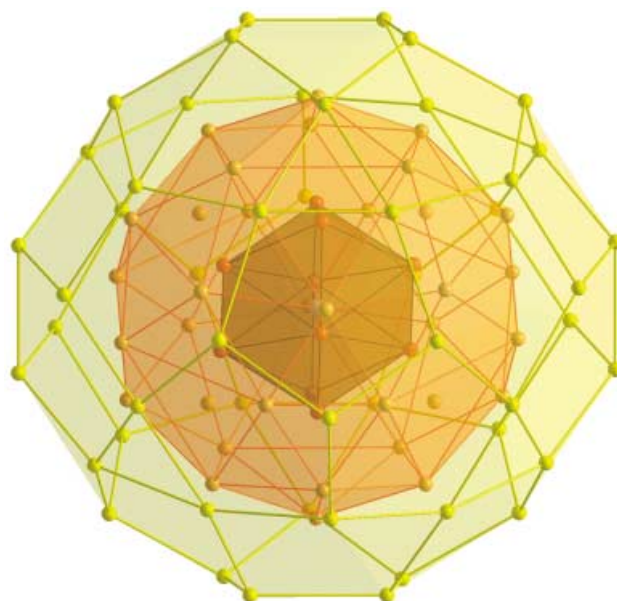


Figure 4. The sulfur substructure in **2**. The central S₁₀ polyhedron (orange) is surrounded by a S₃₄ polyhedron (dark yellow) which itself is encapsulated by a S₅₀ polyhedron (bright yellow).

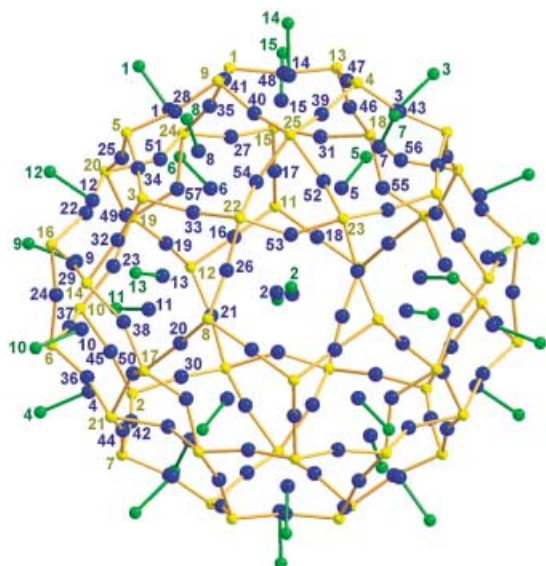


Figure 5. The outer shell of **2** consisting of 114 Ag atoms (blue), 50 S atoms (yellow), and P atoms (green; $PnPr_3$).

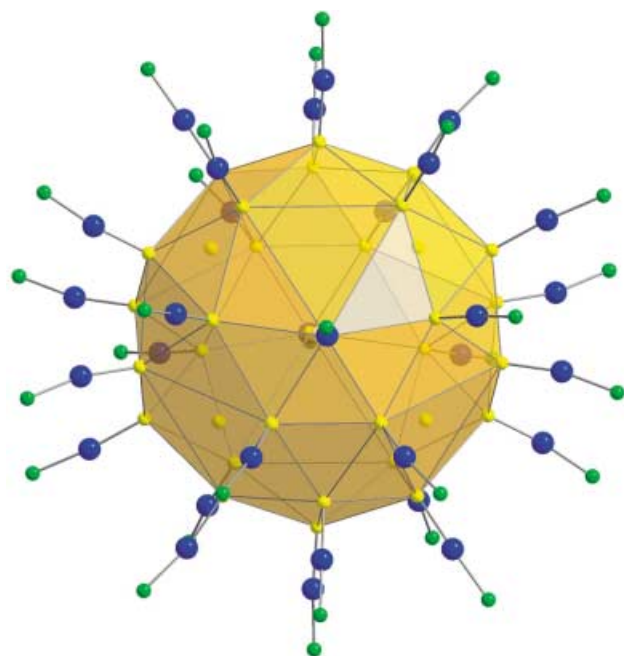


Figure 6. The middle shell in **2** consists of 34 S^{2-} ligands bound to P-coordinated Ag atoms; P (green), S^{2-} ions (yellow), Ag (blue).

the Ag atoms and S atoms located on the $Ag_{114}S_{50}$ cluster surface ($Ag \cdots Ag > 297$ pm, $Ag \cdots S$ 327–418 pm).

The atoms Ag58–Ag64 connect the outer with the middle shell. Each one of these Ag atoms is coordinated by one S atom of the outer S_{50} shell and two S atoms of the middle S_{34} shell and has a distorted trigonal-planar coordination geometry (Ag–S 258.1(6)–294.7(7) pm, S–Ag–S 102.3(2)–145.9(2)°, Σ S–Ag–S 358.5–360°). Ag62–Ag64 occupy vacant tetrahedral positions located between both S polyhedra (Ag–S 261.4(6)–293.9(6) pm). The atoms Ag65 and Ag66 are solely coordinated by S atoms of the middle S_{34} shell in a distorted linear fashion (Ag–S 250.7(5)–257.9(6) pm, S–Ag–S 147.8(2)–

161.4(2)°). Ag67–Ag80 are coordinated by three S atoms belonging to the middle S_{34} polyhedra and have a distorted trigonal-planar coordination geometry (Ag–S 256.1(6)–274.4(6) pm, S–Ag–S 101.6(2)–126.3(2)°, Σ S–Ag–S 336.5–349.8°).

Ag81–Ag94 act as bridging atoms between the middle S_{34} and the inner S_{10} polyhedron. Ag81 and Ag82 are coordinated by two S atoms (Ag–S 255.1(6)–262.4(6) pm, S–Ag–S 172.3(3)°) in a slightly bent arrangement. Ag83–Ag89 show a distorted trigonal-planar coordination (Ag–S 242.1(6)–287.1(8) pm, S–Ag–S 83.2(2)–163.6(3)°, Σ S–Ag–S 353.3–359.8°). Distorted tetrahedral coordination is observed for Ag90–Ag94 (Ag–S 251.7(9)–280.2(7) pm). As a result, the middle shell (diameter 1.1–1.5 nm) is formed by S26–S42, Ag58–Ag80, Ag81 and Ag83 and has the formula $Ag_{50}S_{34}$ (Figure 7). Ag82 and Ag84–Ag94 connect the middle shell with the inner S_{10} polyhedron. Ag49–Ag57 connect the $Ag_{114}S_{50}$ outer shell through Ag–S bonds with the $Ag_{50}S_{34}$ middle shell (Ag–S > 302 pm).

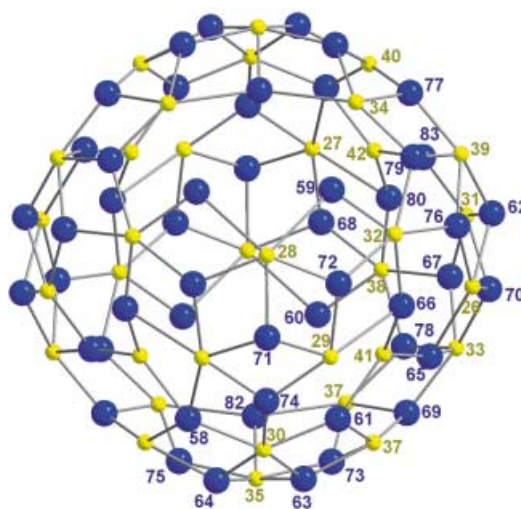


Figure 7. Spherical structure of the middle shell $Ag_{50}S_{34}$ S^{2-} ions (yellow), Ag (blue) in **2**.

The S^{2-} ions in **2** adopt various coordination modes. S1–S16 act as μ_3 bridging ligands coordinating three Ag^+ ions each (Ag–S–Ag 63.2(2)–115.5(3)°). S17–S25 are μ_4 bridging and each coordinate four Ag^+ ions of the outer $Ag_{114}S_{50}$ shell. Weak Ag–S interactions to Ag^+ ions belonging to the inner shell lead to distorted tetrahedral geometry for S1–S16 and distorted square-planar geometry for S17–S25 ((S1–S16)···Ag 290–312 pm, (S17–S25)···Ag 284–307 pm). The effect of these interactions is that the atoms S1–S25 are around 90–100 pm below the plane of the sulfur-bound Ag ions.

Of the 34 sulfide ions (S26–S42) of the middle S_{34} polyhedron 30 coordinate atoms Ag1–Ag15, each of these sulfide ions is surrounded by a distorted octahedron of six Ag^+ ions. The same coordination mode is found for S43, S44, and S46. Only S45 and S46 form μ_4 bridges.

So far we have assumed that Ag–S bonds are covalent. However, one must not overlook—the important!—ionic interactions between Ag^+ and S^{2-} ions. In an alternative

approach **2** could be described as an uncharacteristic nanoparticle of a crystal with the ionic Ag_2S structure. The formation of **2** instead of Ag_2S occurs because of the presence of the protecting ligand sphere.

Other silver chalcogenide clusters synthesized in our group all show the phenomenon of increased Ag disorder with increasing cluster size. This observation is in agreement with the fact that nanoparticles of the composition Ag_2E generally show a higher degree of Ag disorder than the corresponding binary crystalline phases. Similar disorder has also been observed in the isostructural cluster core of **3**. This suggests that the choice of cluster-stabilizing tertiary phosphane ligands does not effect the disorder within these Ag_2S clusters.

Experimental Section

All experiments were carried out under exclusion of oxygen and moisture in an atmosphere of dry nitrogen.

1: $\text{S}(\text{Ph})\text{SiMe}_3$ (0.10 mL, 0.50 mmol) and $\text{S}(\text{SiMe}_3)_2$ (0.04 mL, 0.25 mmol) is added a rapidly stirred suspension of PhCO_2Ag (silver benzoate; 230 mg, 1.00 mmol) and triphos (100 mg, 0.25 mmol) in diglyme (20 mL) at -20°C . The reaction was then allowed to slowly warm to 0°C . After 2 h at 0°C the reaction mixture was allowed to warm to room temperature. Storage of the reaction for one month produced tiny red needles of **1** (yield 27%).

2: $\text{CF}_3\text{CO}_2\text{Ag}$ (silver trifluoroacetate; 230 mg, 1.00 mmol), PnPr_3 (0.2 mL, 1.00 mmol), and $\text{S}(\text{SiMe}_3)_2$ (0.08 mL, 0.50 mmol) in diglyme (20 mL) were stirred at -40°C . After 2 h the reaction was allowed to warm to room temperature. Storage of the reaction mixture for seven days produced black crystals of **2** (33%). Changes to the reaction conditions causes precipitation of **2** and AgS as a black powder.

3: $\text{S}(\text{SiMe}_3)_2$ (0.08 mL, 0.50 mmol) was added to a suspension of $\text{CF}_3\text{CO}_2\text{Ag}$ (230 mg, 1.00 mmol) and PnBu_3 (0.25 mL, 1.00 mmol) in diglyme (25 mL) at -40°C . After 3 days at this temperature the deep red solution was allowed to warm to -20°C , then, after 1 day at this temperature, the reaction was allowed to warm to room temperature. Black crystals of **3** were formed on storing the reaction mixture at room temperature for 1 week.

Correct elemental analyses (C, H, O, P, Ag) for **1–3** were obtained.

Received: May 8, 2002 [Z19271]

- [1] A. Müller, E. Beckmann, H. Bögge, M. Schmidtman, A. Dress, *Angew. Chem.* **2002**, *114*, 1210–1215; *Angew. Chem. Int. Ed.* **2002**, *41*, 1162–1167.
- [2] N. T. Tran, D. R. Powell, L. F. Dahl, *Angew. Chem.* **2000**, *112*, 4287–4291; *Angew. Chem. Int. Ed.* **2000**, *39*, 4121–4125.
- [3] A. Schnepf, H. Schnöckel, *Angew. Chem.* **2001**, *113*, 734–737; *Angew. Chem. Int. Ed.* **2001**, *40*, 711–715.
- [4] X. Jin, K. Tang, W. Liu, H. Zeng, H. Zhao, Y. Ouyang, Y. Tang, *Polyhedron* **1996**, *15*, 1207–1211.
- [5] K. Tang, X. Xie, Y. Zhang, X. Zhao, X. Jin, *Chem. Commun.* **2002**, 1024–1026.
- [6] S. Dehnen, A. Eichhöfer, D. Fenske, *Eur. J. Inorg. Chem.* **2002**, 269–275.
- [7] a) A. Eichhöfer, D. Fenske, H. Pfister, M. Wunder, *Z. Anorg. Allg. Chem.* **1998**, *624*, 1909–1914; b) M. Semmelmann, D. Fenske, J. F. Corrigan, *J. Chem. Soc. Dalton Trans.* **1998**, 2541–2546; c) S. Behrens, D. Fenske, *Ber. Bunsen-ges.* **1997**, *101*, 1588–1592; d) J. F. Corrigan, D. Fenske, *Angew. Chem.* **1997**, *109*, 2070–2072; *Angew. Chem. Int. Ed. Engl.* **1997**, *36*, 1981–1983; e) J. F. Corrigan, D. Fenske, *Chem. Commun.* **1997**, 1837–1838; f) S. Dehnen, D. Fenske, *Chem. Eur. J.* **1996**, *2*, 1407–1416; g) D. Fenske, J. Ohmer, J. Hachgenei, K. Merzweiler, *Angew. Chem.* **1988**, *100*, 1300–1320; *Angew. Chem. Int. Ed. Engl.* **1988**, *27*, 1277–1297.
- [8] a) S. Dehnen, A. Schäfer, D. Fenske, R. Ahlrichs, *Angew. Chem.* **1994**, *106*, 786–790; *Angew. Chem. Int. Ed. Engl.* **1994**, *33*, 746–748; b) A. Schäfer, R. Ahlrichs, *J. Am. Chem. Soc.* **1994**, *116*, 10686–10692; c) S. Dehnen, A. Schäfer, R. Ahlrichs, D. Fenske, *Chem. Eur. J.* **1996**, *2*, 429–435.
- [9] H. Krautscheid, D. Fenske, G. Baum, M. Semmelmann, *Angew. Chem.* **1993**, *105*, 1364–1367; *Angew. Chem. Int. Ed. Engl.* **1993**, *32*, 1303–1306.
- [10] D. Fenske, N. Zhu, T. Langetepe, *Angew. Chem.* **1998**, *110*, 2783–2788; *Angew. Chem. Int. Ed.* **1998**, *37*, 2639–2644.
- [11] T. Langetepe, D. Fenske, *Z. Anorg. Allg. Chem.* **2001**, *627*, 820–824.
- [12] D. Fenske, T. Langetepe, M. M. Kappes, O. Hampe, P. Weis, *Angew. Chem.* **2000**, *112*, 1925–1928; *Angew. Chem. Int. Ed.* **2000**, *39*, 1857–1860.
- [13] H. Pfister, D. Fenske, *Z. Anorg. Allg. Chem.* **2001**, *627*, 575–582.
- [14] D. van der Putten, D. Olevano, R. Zanon, H. Krautscheid, D. Fenske, *J. Electron Spectrosc. Relat. Phenom.* **1995**, *76*, 207–211.
- [15] X-ray analysis: STOE-IPDS II (MoK_α); data collection and refinement (SHELX97, SHELXL93); empirical absorption correction (HABITUS). CCDC-187700 (**1**) and 187701 (**2**) contains the supplementary crystallographic data for this paper. These data can be obtained free of charge via www.ccdc.cam.ac.uk/conts/retrieving.html (or from the Cambridge Crystallographic Data Centre, 12, Union Road, Cambridge CB2 1EZ, UK; fax: (+44) 1223-336-033; or deposit@ccdc.cam.ac.uk). **1:** $\text{C}_{376}\text{H}_{346}\text{Ag}_{70}\text{O}_8\text{P}_{12}\text{S}_{50}\cdot 2$ diglyme, triclinic, space group $\bar{P}1$ (no 2); $Z=2$, (150 K): $a=2546.0(5)$, $b=2915.6(6)$, $c=3946.0(8)$ pm, $\alpha=91.16(3)^\circ$, $\beta=96.63(3)^\circ$, $\gamma=113.93(3)^\circ$, $V=26522.5\times 10^6$ pm³, $\mu(\text{MoK}_\alpha)=2.8$ mm⁻¹, $2\theta_{\text{max}}=55^\circ$, of a total of 192662 reflections collected, 109402 were independent and 109317 reflections with $I>2\sigma(I)$, 3149 parameters (Ag, S, P anisotrope, O, C isotrope). Maximum residual electron density $2.8\text{ e}\cdot\text{\AA}^{-3}$, $R1=0.113$; $wR2=0.319$. **2:** $\text{C}_{270}\text{H}_{630}\text{Ag}_{188}\text{P}_{30}\text{S}_{94}\cdot 2$ diglyme, triclinic, space group $\bar{P}1$ (no 2), $Z=1$, (150 K): $a=2714.7(5)$, $b=2825.7(4)$, $c=28494(5)$ pm, $\alpha=119.05(2)^\circ$, $\beta=91.28(1)^\circ$, $\gamma=117.86(2)^\circ$, $V=15991.3\times 10^6$ pm³, $\mu(\text{MoK}_\alpha)=6.0$ mm⁻¹, $2\theta_{\text{max}}=57^\circ$, of a total of 118990 collected, 62257 were independent and 47327 reflections with $I>2\sigma(I)$, 2254 parameters (Ag, S, P anisotrope, C isotrope), Cancellation effects in the inside of the cluster were refined as Ag atoms (occupation 0.25). Maximum residual electron density $6.9\text{ e}\cdot\text{\AA}^{-3}$, $R1=0.098$; $wR2=0.241$. High residual electron density is located between S_{34} and S_{10} polyhedra and inside the S_{10} polyhedron. A more accurate allocation is impossible. These positions could be partially occupied by $\text{Ag}_{87}\text{–Ag}_{94}$.
- [16] G. A. Wieggers, *Am. Mineral.* **1971**, *56*, 1882–1888; Z. G. Pinsker, C. Chianliang, R. M. Imamov, E. L. Lapidus, *Sov. Phys. Crystallogr. Engl. Transl.* **1965**, *7*, 225–233.
- [17] a) S. Dehnen, A. Eichhöfer, D. Fenske, *Eur. J. Inorg. Chem.* **2002**, 279–318; b) V. Soloviev, A. Eichhöfer, D. Fenske, U. Banin, *J. Am. Chem. Soc.* **2000**, *122*, 2673–2674; c) V. Soloviev, A. Eichhöfer, D. Fenske, U. Banin, *J. Am. Chem. Soc.* **2001**, *123*, 2354–2364; d) N. Zhu, D. Fenske, *J. Chem. Soc. Dalton Trans.* **1999**, 1067–1076; e) A. Eichhöfer, D. Fenske, *J. Chem. Soc. Dalton Trans.* **1998**, 2969–2972; f) A. C. Deveson, S. Dehnen, D. Fenske, *J. Chem. Soc. Dalton Trans.* **1997**, 4491–4498; g) S. Behrens, M. Bettenhausen, A. Eichhöfer, D. Fenske, *Angew. Chem.* **1997**, *109*, 2874–2876; *Angew. Chem. Int. Ed. Engl.* **1997**, *36*, 2797–2799; h) S. Behrens, M. Bettenhausen, A. C. Deveson, A. Eichhöfer, D. Fenske, A. Lohde, U. Woggon, *Angew. Chem.* **1996**, *108*, 2361–2364; *Angew. Chem. Int. Ed. Engl.* **1996**, *35*, 2215–2218; i) S. Dehnen, D. Fenske, A. C. Deveson, *J. Cluster Sci.* **1996**, *3*, 351–369; j) S. Dehnen, D. Fenske, *Angew. Chem.* **1994**, *106*, 2369–2372; *Angew. Chem. Int. Ed. Engl.* **1994**, *33*, 2287–2289; k) D. Fenske, H. Krautscheid, *Angew. Chem.* **1990**, *102*, 1513–1516; *Angew. Chem. Int. Ed. Engl.* **1990**, *29*, 1452–1454; l) D. Fenske, J. Ohmer, J. Hachgenei, *Angew. Chem.* **1985**, *97*, 993–995; *Angew. Chem. Int. Ed. Engl.* **1985**, *24*, 993–995.
- [18] D. Fenske, T. Langetepe, *Angew. Chem.* **2002**, *14*, 306–310; *Angew. Chem. Int. Ed.* **2002**, *41*, 300–304.